COBEM 2021 26th International Congress of Mechanical Engineering
November 22-26, 2021, Virtual Congress, Brazil

COB-2021-1561
Fretting fatigue of 6201 aluminum alloy wires under variable amplitude loading: An initial study

Ian de Medeiros Matos
200078569@aluno.unb.br
José Alexander Araújo
alex07@unb.br
Fábio Comes de Castro
fabiocastro@unb.br
Department of Mechanical Engineering, University of Brasilia, 70910-900 Brasilia, DF, Brazil

Abstract. *This study investigates the fretting behavior of 6201-T81 aluminum alloy wires taken from an AAAC 900 MCM conductor. New variable amplitude loading fretting fatigue tests on a wire/wire contact configuration were proposed. In these tests, the amplitude variation is represented by loading blocks with three sub-blocks of different amplitudes. A finite element-based life estimation methodology was implemented to predict the fatigue lives of the wires. The methodology uses an average stress over a fatigue damage zone to consider the stress gradients beneath the contact and the Smith–Watson–Topper parameter to quantify the fatigue damage. In previous studies, this methodology was employed to predict the fatigue lives of wires under fretting conditions when subjected to constant amplitude fatigue loadings. In this study, the methodology was extended for problems with variable amplitude loading, using the Rainflow method for cycle counting and Miner's damage rule to estimate the cumulative fatigue damage. The fatigue life estimates were in a range of 1.5 to 4 million cycles. The magnitude of the highest force amplitude had a significant effect on the life estimates. Wire/wire tests with the proposed load conditions are still required to properly evaluate the accuracy of the methodology.*

Keywords: *overhead conductor, alumium wire, fretting fatigue, variable amplitude loading, life prediction.*

1. INTRODUCTION

The fatigue failure of overhead conductors is a critical problem for transmission lines. Usually, the failure is caused by aeolian vibrations, which induce minute relative displacements between wires in contact with each other or with devices installed in the transmission line. The process of surface damage caused by these minute displacements is known as fretting and it can be critical to wire ruptures in overhead conductors (EPRI, 2006). The failure usually takes place near components that restrain the movement of the conductor, such as spacers and suspension clamps (Cardou et al., 1992; Zhou et al., 1994). In these critical regions, the wires are subjected to aeolian vibrations and static loads due to clamping pressure, stretching load and weight of the conductor. This load combination favors crack initiation and propagation, eventually leading to wire rupture. Field (Kalombo et al., 2015; Azevedo and Cescon, 2002) and laboratory (Fadel et al., 2012; Azevedo et al., 2009) researches have indicated a clear correlation between fretting fatigue and wire rupture in overhead conductors.

The safety design and operation of overhead conductors is usually based on data obtained from fatigue tests with conductors. These are generally performed on test benches (Fadel et al., 2012; Azevedo et al., 2009; Ouaki et al., 2003), where a conductor-clamp system is subjected to constant amplitude oscillations used to represent the in-field aeolian vibrations. Recent advancements in numerical simulation tools have lead researchers to develop three-dimensional finite element-based models of the conductor-clamp assembly (Lalonde et al., 2018; Baumann and Novak, 2017), in order to investigate the flexural stiffness, potential crack initiation sites, and stresses and strains acting on conductors subjected to combined tension and cyclic bending loads. In addition to the global-scale analyzes of the conductor-clamp system, recent researches have tried to investigate the fatigue failure of conductors on a local (wire) scale. In such studies, fretting tests and finite element simulations are performed to reproduce the fretting conditions at the contact between wires of adjacent layers (Said et al., 2020; Matos et al., 2020; Rocha et al., 2019) or between a wire of the external layer of the conductor with a clamp device (Omrani et al., 2021; Steier et al., 2018).

Most of the experimental and numerical studies on the fatigue behavior of the conductor consider constant amplitude vibrations. However, field measurements indicate that the conductor oscillation has a variable amplitude nature, often following a beat pattern (EPRI, 2006; Noiseux et al., 1987). Figure 1 shows a sample of vibration data recorded from an actual transmission line, exemplifying the beat pattern. It may be worthwhile to investigate the effect of amplitude

variation on the fatigue behavior of overhead conductors by means of local scale fretting analyzes. In this context, the present work aims at developing methodology to predict the fatigue lives of wires under fretting conditions. In previous studies (Rocha et al., 2019; Matos et al., 2020), this methodology was designed and applied for wires subjected to constant amplitude loadings. In this work, the methodology is extended for variable amplitude loading conditions and is applied to estimate the fatigue lives of 6201-T81 aluminum alloy wires subjected to variable amplitude loadings.

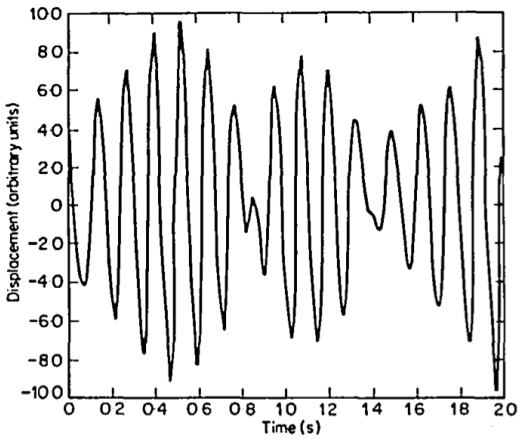

Figure 1. Sample of transmission line vibration data. Figure taken from (Noiseux et al., 1987).

2. FRETTING FATIGUE TESTS ON A WIRE/WIRE CONTACT CONFIGURATION

In a previous study (Matos et al., 2020), fretting fatigue tests with constant amplitude loading (CAL) were performed on 6201-T81 aluminum alloy (AA) wires taken from an AAAC 900 MCM conductor. The tests were carried out on a custom-designed apparatus, mounted on an MTS testing machine. Details about the design and operation, and performance tests on the device can be found in (Garcia et al., 2020). Using this apparatus, it is possible to perform fatigue tests on crossed wires, representing the contact between wires of adjacent layers of an overhead conductor. Figure 2a shows the contact configuration of two wires and a bearing, which is used to resist the compressive force. Figures 2b and c show an schematic of the applied loads and loading history of the fretting fatigue tests. Initially an axial mean force, F_m, is applied to the specimen (vertical wire). Then a normal force, P, is used to compress the pad (tilted wire) and the bearing against the specimen. This force is kept constant throughout the test. Finally, the force applied to the specimen is cycled with a constant amplitude, $\Delta F/2$. Table 1 summarizes the test conditions applied in the fretting tests and the fatigue lives of the wires, N_f, defined as the number of cycles to the complete rupture of the specimen into two parts.

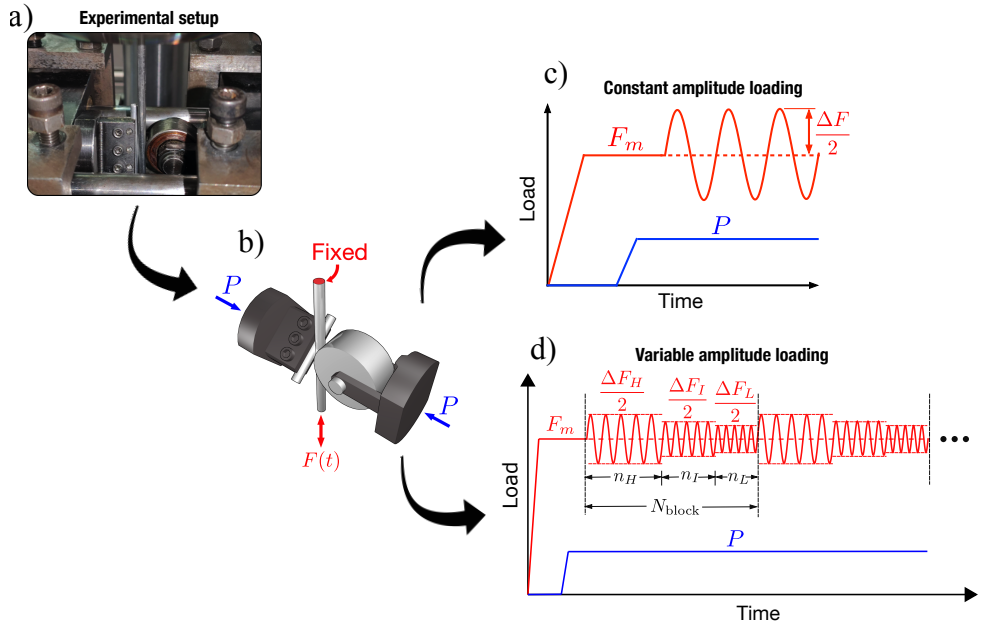

Figure 2. (a) Experimental setup of a fatigue test with fretting wires, (b) schematic of the loads applied in the test and loading history for the fretting test simulations under (c) constant amplitude and (d) variable amplitude loadings.

Table 1. Test data from the fretting fatigue tests with constant amplitude loading.

Load condition	P [N]	F_m [N]	$\Delta F/2$ [N]	N_f [cycles]
CAL01	500	3150	292	9.85×10^5
CAL02	500	2990	292	1.35×10^6
CAL03	500	2990	292	1.57×10^6
CAL04	500	2800	292	2.84×10^6
CAL05	500	2600	292	$> 5.00 \times 10^6$
CAL06	500	2490	292	$> 5.00 \times 10^6$
CAL07	750	3150	292	4.61×10^6
CAL08	750	3150	292	4.77×10^6
CAL09	750	2990	292	1.15×10^7

In this study, a new set of fretting fatigue tests with variable amplitude loading (VAL) is proposed. To describe the amplitude variation, loading blocks that repeat periodically are used and each block is composed of three sub-blocks with different amplitudes. Figure 2d represents the loading history for these tests. As in the tests with constant amplitude loading, a mean force, F_m, is used to stretch one of the wires and a normal force, P, is used to compress the wires into each other. The only difference is the use of loading blocks with three sub-blocks. The amplitude of the fatigue force, $\Delta F/2$, and the number of cycles, n, applied to each sub-block are identified with subscripts H, I and L, which refer to the high, intermediate and low force amplitudes applied, respectively. The use of loading blocks allows a simple representation of the amplitude variations the conductor may have during operation. In previous studies (Goudreau et al., 2005; Brunair et al., 1988; Ramey and Silva, 1981), loading blocks were used in fatigue tests of conductors to investigate the effect of variable amplitude loading on fatigue life.

A key point in planning the VAL wire/wire tests is the selection of loading and contact conditions that are representative of the fretting fatigue in overhead conductors. These conditions are the crossing angle between the wires and the loads applied during the tests, as represented in Fig. 2d. In this work, the crossing angle, α, and the magnitudes of the normal force, P, and the mean force, F_m, were estimated based on an experimental-numerical procedure by Rocha (2019). The experimental part consisted of fatigue tests performed on an AAAC 900 MCM conductor on a 47 m resonant test bench. These tests were used to estimate the bulk stresses on wires of the external layer of the conductor after applying a stretching force and during the fatigue loading. The numerical part consisted of finite element simulations of the contact between wires of adjacent layers, which were used to estimate the normal force necessary to reproduce the dimensions of the contact marks observed experimentally. The crossing angle, α, observed between wires of the two outermost layers of the conductor was 20º. The magnitudes of the normal contact force, P, were observed to range from 100 to 1280 N. Mean bulk stresses ranging from 202 to 256 MPa were estimated, resulting in mean forces, F_m, of 2470 to 3150 N. Based on these results, a normal force $P = 500$ N and a mean force $F_m = 2990$ N were chosen for the VAL tests.

The force amplitudes applied in each sub-block were estimated based on the vibration measurements of a 230 kV transmission line located at the Center-West of Brazil, as reported in (Kalombo et al., 2015). To investigate premature failures of the conductor, vibration recorders were installed on spacer clamps at two spans of the line. The recorders registered the bending amplitudes, Y_b, of the conductor and the number of cycles in each amplitude for a period of ten days. Results were extrapolated to a period of one year and are represented in Fig. 3a for one of the spans. The bending amplitudes were then associated with bending stress amplitudes, σ_a, at wires of the external layer of the conductor using the well-known Poffenberger-Swart equation (Poffenberger and Swart, 1965), which can be expressed as $\sigma_a = KY_b$. Parameter K is a function of the material and geometry of the conductor and the tension applied. For the referred line, $K = 35$ MPa/mm. Finally, the force amplitudes, $\Delta F/2$, can be estimated as $\Delta F/2 = M\sigma_a A_w$, where M is a multiplying factor and A_w is the area of the cross section of a wire from the external layer. For the AAAC 900 MCM conductor, $A_w = 12.32$ mm^2. It is worth noticing that the measured bending amplitudes shown in Fig. 3a are very small, resulting in small magnitudes of the force amplitudes when $M = 1$. This result is expected since the conductor is designed to operate over hundreds of millions of cycles. To define test conditions that can be performed within a reasonable time frame, a multiplying factor $M = 3$ was used in this work to estimate the force amplitudes. The final estimates are represented in the force amplitude vs. megacycles per year curve shown in Fig. 3b, which was used to define the loading conditions of the VAL tests shown in Table 2. To define the force amplitude of the sub-blocks, three points are chosen from this curve. Note that most of the loading cycles occur at smaller amplitudes, which was taken into consideration when defining the the number of cycles, n, of each sub-block. For this study, the force amplitudes of the intermediate and low sub-blocks and the number of cycles of the sub-blocks were kept constant in all test conditions. The force amplitudes defined for the high sub-block were chosen to represent stress levels that occur for a very short amount of cycles compared to the total lifetime of the conductor. Despite their short duration, the highest stress (or strain) amplitudes are commonly used in the industry to evaluate the risk of fatigue failure in endurance limit criteria. In a future study, new finite element simulations

and fretting fatigue tests will be performed under similar conditions, but changing the lowest force amplitude in each test. The idea is to evaluate which force amplitude is more significant to the fretting fatigue of the wires: the highest amplitude that occurs during few cycles, or the lowest amplitude that occurs during most of the conductor's lifetime.

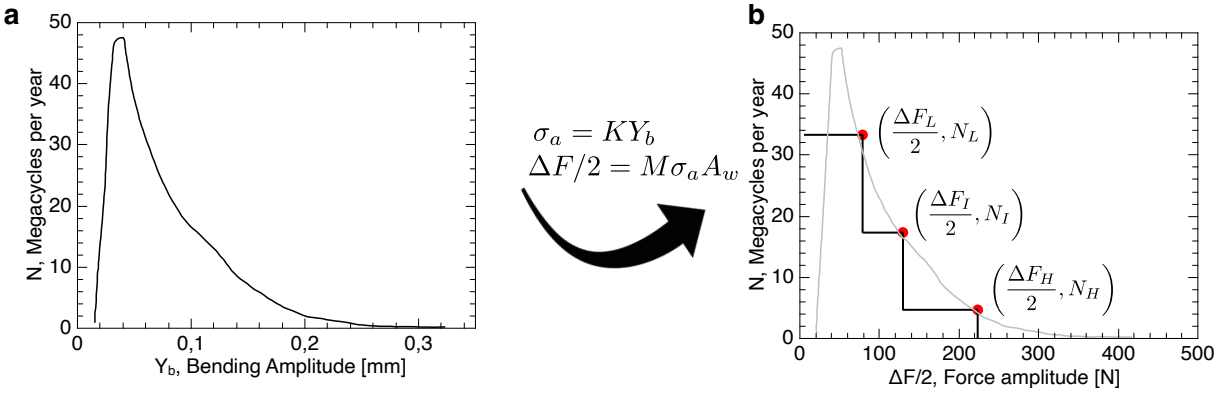

Figure 3. Number of megacycles per year of an AAAC 900 MCM conductor vs. (a) the bending amplitudes and (b) the corresponding force amplitudes.

Table 2. Test conditions for fretting fatigue tests with variable amplitude loading.

Load condition	P [N]	F_m [N]	$\Delta F_H/2$ [N]	$\Delta F_I/2$ [N]	$\Delta F_L/2$ [N]	n_H [cycles]	n_I [cycles]	n_L [cycles]
VAL01	500	2990	493	296	197	2500	7500	40,000
VAL02	500	2990	443	296	197	2500	7500	40,000
VAL03	500	2990	394	296	197	2500	7500	40,000
VAL04	500	2990	345	296	197	2500	7500	40,000

3. METHODOLOGY FOR LIFE PREDICTION

This section describes a methodology for life prediction of wires under fretting conditions. The methodology was developed based on the similarities shared between notches and fretting wires, such as the presence of stress concentration, stress gradient, localized plastic strains and multiaxial state of stress. Based on this analogy, Rocha et al. (2019) proposed a life estimation methodology for fretting wires, initially applied by the authors to 1350-H19 aluminum alloy (AA) wires and later (Matos et al., 2020) to AA6201-T81 wires. In both of these studies, the analyzes were limited to wires subjected to constant amplitude fatigue loadings. In what follows, an extension of the life estimation methodology is proposed to account for variable amplitude loading conditions.

The life estimation methodology used in this study is based on the Theory of Critical Distances (TCD). According to this theory, the material failure happens when the damage accumulated over a process zone reaches a critical value. For the volume method of the TCD, an average stress tensor, $\boldsymbol{\sigma}$, over a process zone can be defined as

$$\boldsymbol{\sigma} = \int_V \hat{\boldsymbol{\sigma}} dV \tag{1}$$

where $\hat{\boldsymbol{\sigma}}$ is the stress tensor of a point within the volume V of the process zone. In this work, a semi-spherical damage zone with radius L is used, and the center of the flat side of this zone is located at the hotspot.

The fretting fatigue of wires produces a multiaxial stress state beneath the contact zone. Among the fatigue parameters used to evaluate the damage produced in such a state are those based on the concept of critical planes, such as the models of Findley, Fatemi–Socie and Smith–Watson–Topper (SWT). These critical plane models are based on the physical observation that cracks initiate and propagate on preferred material planes. For the following analyzes, the orientation of a material plane will be defined by a pair of angles (θ, ϕ), where angle θ indicates the surface crack orientation and angle ϕ indicates the inclination of the crack. A stress-based version of the SWT parameter is used in the present work. This parameter was previously employed in the analyzes of fretting wires under constant amplitude loading (Matos et al., 2020; Rocha et al., 2019) and typically performs well for aluminum alloys (Dowling et al., 2009). In this study, the SWT parameter is defined as

$$\text{SWT} = \sqrt{\sigma_{\text{na}} \langle \sigma_{\text{nmax}} \rangle} = A N_f^b \tag{2}$$

where σ_{na} and σ_{nmax} are the normal stress amplitude and the maximum normal stress in a loading cycle, respectively, and N_f is the number of cycles to failure. The Macaulay brackets $\langle\rangle$ are used to ensure that no damage is produced if the maximum normal stress is compressive. The material constants A and b can be obtained by fitting S-N test data of smooth specimens.

For variable amplitude loadings, a cycle-counting method may be required to determine the stress quantities σ_{na} and σ_{nmax} shown in Eq. (2). In the proposed life estimation methodology, the Rainflow cycle-counting method is used. Considering that the spectrum of the normal stress can be represented by one loading block repeated periodically, the use of the Rainflow method provides k different combinations of normal stress amplitude and maximum normal stress, each being repeated for N_j cycles. Thus, the number of cycles of the loading block, N_B, can be defined as

$$N_B = \sum_{j=1}^{k} N_j \tag{3}$$

Eq. (2) can then be used to estimate an SWT parameter for each combination of normal stress amplitude and maximum normal stress obtained with the Rainflow method.

The strategy used to define the critical plane is based on Miner's cumulative damage rule (Miner, 1945). The fatigue damage, $\Delta D(\theta, \phi)$, produced by one loading block with k different magnitudes of the SWT parameter can be defined as

$$\Delta D(\theta, \phi) = \sum_{j=1}^{k} \frac{N_j}{N_{f_j}} \tag{4}$$

where N_j is the number of cycles counted for each magnitude of the SWT parameter and N_{f_j} is the number of cycles to failure, obtained using the SWT–N_f relation. The critical plane (θ_c,ϕ_c) can then be determined as the plane that maximizes the damage produced during one loading block. The equivalent number of cycles to failure, $N_{f,eq}$, is defined as the number of cycles required to reach a critical damage, D_c, and can be expressed as

$$N_{f,eq} = D_c \frac{N_B}{\Delta D(\theta_c, \phi_c)} \tag{5}$$

In this study, all life estimates are obtained using $D_c = 1$.

The use of fatigue criteria based on the TCD relies on estimating the critical distance, L, which is related to the size of the process zone. According to Susmel and Taylor (2007), it is possible to associate the critical distance with the fatigue life, which can be achieved by using a power-law function, such as

$$L = C N_f^d \tag{6}$$

where C and d are material constants obtained by fitting S-N test data of sharply notched specimens.

Susmel and Taylor (2012) showed that the constants C and d in Eq. (6) can be obtained from fully reversed axial test data and provide reasonable fatigue life estimates, even when estimating the lives of components subjected to variable amplitude loadings. Considering that, the procedure used in this work to determine the constants of the L-N_f relation is the same one used by Rocha et al. (2019) and Matos et al. (2020), which can be summarized as follows. The input data for this procedure consists of test data from smooth and notched specimens. Initially, the test data from the smooth specimens are used to determine the constants A and b of the SWT-N_f relation, Eq. (2). Then one point from the experimental data of the notched specimens is selected to determine a pair of stress amplitude, $\Delta S/2$, and observed fatigue life, N_{obs}. An initial estimate is made for the critical distance, L_{trial}, which defines the radius of the semi-spherical process zone, whose center of the flat side is positioned at the notch root. A stress analysis of the notched specimen is performed and the average stress tensor over the process zone is estimated using Eq. (1). For each material plane (θ, ϕ), the SWT parameter and the fatigue life can be estimated using Eq. (2) and the critical plane is defined as the plane that maximizes the SWT parameter. If the life estimated using the SWT parameter at the critical plane is different than the observed life, the procedure is repeated with a new estimate for the critical distance, L_{trial}, until convergence occurs. At the end of the process, one pair of (L, N_{obs}) is obtained. The procedure is repeated for the remaining test data of the notched specimen and a pair of (L, N_{obs}) is determined for each experimental point. Finally, the set of all pairs of (L, N_{obs}) is fitted by a power-law function to determine the constants of the L-N_f relation, Eq. (6).

The procedure proposed in this work to estimate the fatigue lives of fretting wires under variable amplitude loading is illustrated in Fig. 4. The input data for this procedure are the SWT-N_f and L-N_f curves and the loading conditions on fretting wires, which consist of contact and bulk forces. Initially, an estimate is made for the radius of the semi-spherical process zone, L_{trial}, whose center of the flat side is positioned at the hotspot. Experimental observations (Said et al., 2020; Matos et al., 2020; Rocha et al., 2019) suggest that the hotspot is located at one of the extremities of the major axis of the elliptical contact mark. A stress analysis of the wire/wire contact is performed and the average stress tensor in the process

zone is estimated using Eq. (1). For each material plane (θ, ϕ), the time history of the normal stress is determined for one loading block. Then, the Rainflow method is used for cycle counting, providing k different normal stress amplitudes and maximum normal stresses. Those can be applied in Eq. (2) to obtain k different magnitudes of the SWT parameter and the corresponding number of cycles to failure, N_{f_k}. The damage produced by one loading block can then be determined using Eq. (4) and the critical plane (θ_c, ϕ_c) can be identified as the plane that maximizes this damage. A fatigue life estimate, N_{SWT} is obtained using Eq. (5). A second life estimate, N_L, is obtained by using the estimated critical distance, L_{trial}, in Eq. (6). If $N_{\text{SWT}} \neq N_L$, the procedure is repeated with a new estimate for the critical distance, L_{trial}. The estimated fatigue life, N_{est}, is obtained when the condition $N_{\text{SWT}} = N_L$ is reached.

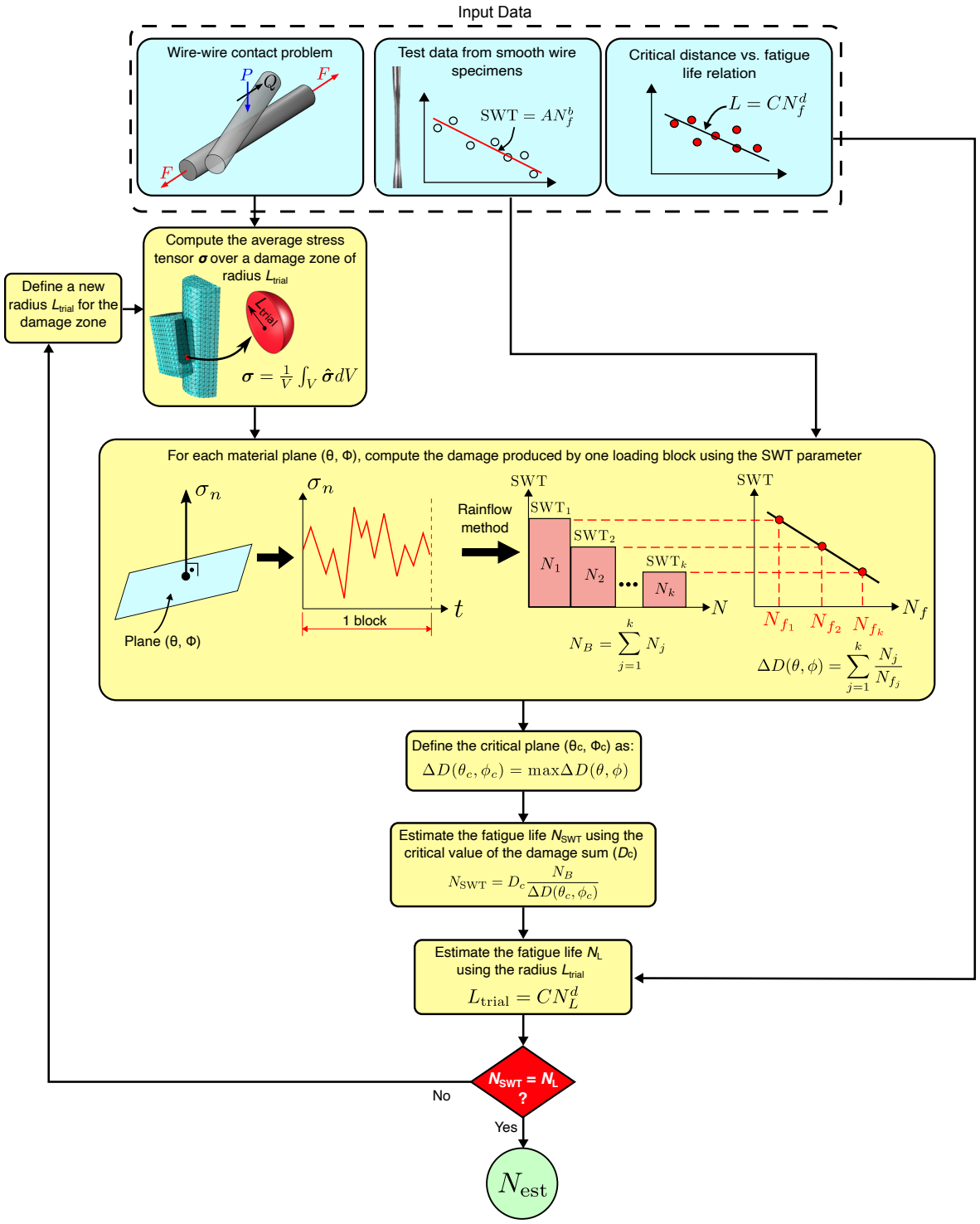

Figure 4. Schematic of the procedure to estimate the fatigue life of fretting wires subjected to variable amplitude fatigue loading.

The life prediction methodology proposed in this work will be used to predict the durability of AA6201-T81 wires subjected to the loading conditions described in Table 2. To implement such a methodology, finite element-based stress analyzes must be performed for notched wires and for the wire/wire contact configuration. The finite element (FE) simulations of notched wires are performed based on the geometry and load conditions shown in (Matos et al., 2020). Details about the FE model can be found in (Rocha et al., 2019). The FE model of the fretting wires is shown in Fig. 5. The specimen and pad are modeled using half-cylinders, placed in contact with each other with a crossing angle of 20º. The contact interaction is defined using finite sliding and surface-to-surface discretization. The tangential behavior of the contact is defined using the penalty formulation, with a friction coefficient of 0.6. An elastic-perfectly plastic material model was used in the FE simulations. A Young's modulus of 69 GPa and a Poisson's ratio of 0.33 were used to define the elastic behavior. The perfectly-plastic behavior was defined using a tensile yield stress of 306 MPa, considering isotropic hardening. These input data were taken from the monotonic stress-strain curve of the material, as shown in (Matos et al., 2020). To properly describe the stress gradient beneath the contact zones, refined partitions were created in the specimen and pad. Eight-node linear brick elements with reduced integration (C3D8R) are used in these partitions, while ten-node quadratic tetrahedral elements (C3D10) are used for the bulk of the wires. The boundary conditions used in the simulations are represented in Fig. 5b, where u is the displacement in the x-y-z coordinate system. Loads were applied as follows; initially, a mean force, F_m, is applied to one end of the specimen, then the normal force, P, is applied to the pad and compresses the wires against each other, and finally the force applied to the specimen is cycled. In the simulations with CAL, four loading cycles with a force amplitude of $\Delta F/2$ are applied, and for the VAL condition, three load cycles are applied at each amplitude.

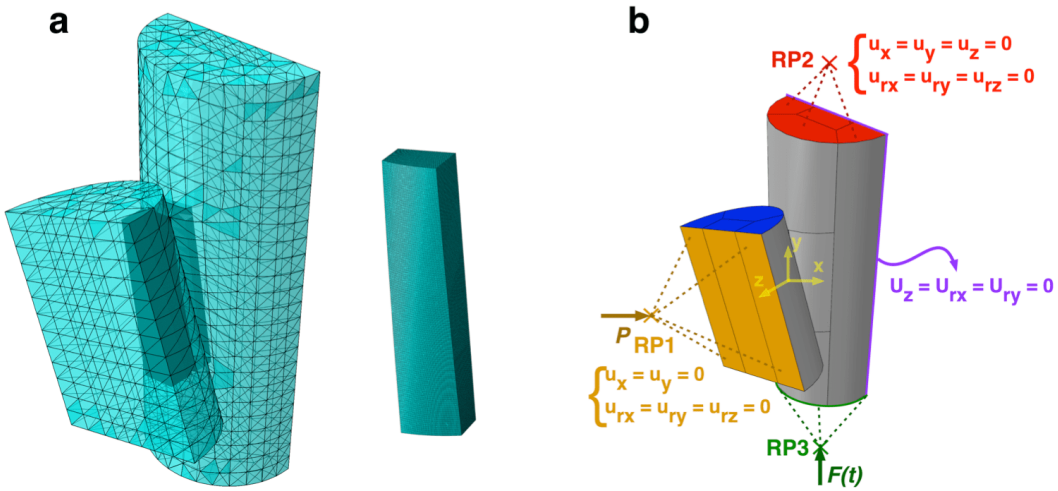

Figure 5. Finite element model of the wires under fretting condition: (a) General view of the model and detail of the refined partition and (b) boundary conditions.

4. RESULTS AND DISCUSSION

4.1 Determination of material constants

To determine the material constants required to apply the life estimation methodology presented in Section 3, fatigue test data from smooth and notched specimens are required. The test data used in this research were previously obtained by Adriano et al. (2018). The tests were performed on smooth and V-notched specimens machined from AA6201-T81 wires taken from an AAAC (All Aluminum Alloy Cable) 900 MCM conductor. The fatigue tests were conducted under fully reversed axial loading. Stress amplitudes, calculated using the minimum cross-sectional area, were in a range of 160 to 180 MPa for the smooth specimens and in a range of 28 to 49 MPa for the V-notched specimens. Tests were carried out until complete rupture of the specimen or were interrupted after 5×10^6 cycles.

Initially, the test data from the smooth wire specimens were used to determine the material constants of the SWT–N_f relation, Eq. 2. The test data were fit by the relation SWT $= 252 N_f^{-0.03}$, as shown in Fig. 6a. Following that, the constants of the L–N_f relation are obtained using the fatigue test data from the V-notched specimens as input data in the calibration procedure described in Section 3. The results shown in Fig. 6b were fit by a power law relation, resulting in $L = 1765 N_f^{-0.24}$

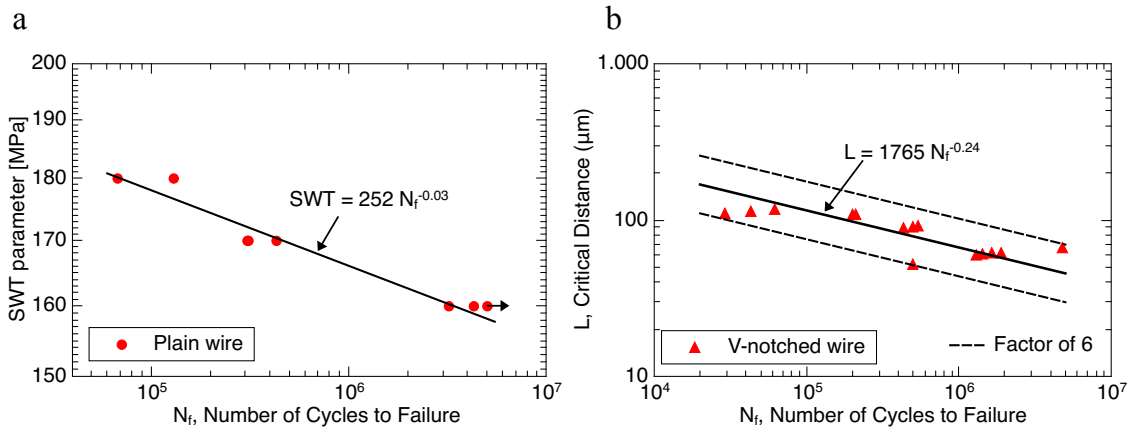

Figure 6. (a) SWT parameter vs fatigue life and (b) critical distance vs fatigue life for the AA6201-T81 wires.

4.2 Fretting fatigue under constant amplitude loading

The material constants of the SWT–N_f and L–N_f relations were used to estimate the fatigue lives of the wires used in the fretting fatigue tests under constant amplitude loading described in Table 1. To estimate the stress field used as input data in the life estimation methodology, finite element simulations of the fretting tests were performed. Linear elastic and elastic-perfectly plastic material models were used in the simulations.

The fatigue lives observed during the fretting tests are compared to the life estimates in Fig. 7. Lives estimated using the linear elastic model were excessively conservative. The inclusion of plasticity during the simulations significantly improved the life estimates, which were within factor-of-five boundaries. The life estimation methodology was sensitive to the normal force applied. For the same fatigue loading conditions, longer fatigue lives were estimated for the tests with a normal force of 750 N than for the ones with 500 N. These results are in agreement with the experimental observations. On the other hand, the effect of the mean stress on fatigue life was not properly described by the model. For the same normal contact force, all life estimates were near identical regardless of the mean stress applied.

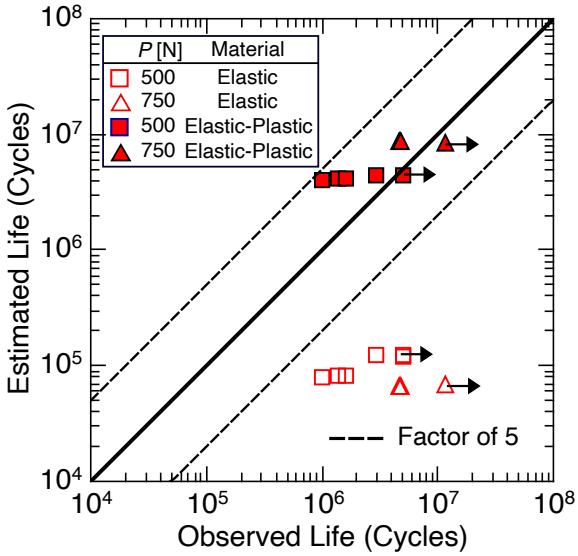

Figure 7. Observed vs estimated fatigue lives for the AA6201-T81 wires subjected to constant amplitude fatigue loadings.

4.3 Fretting fatigue under variable amplitude loading

The life estimation methodology described in Section 3 was applied to predict the fatigue lives of the wires subjected to the variable amplitude loading conditions presented in Table 2. The stress amplitude of the high sub-block vs. estimated fatigue life data is presented in Fig. 8. The life estimates clearly indicate that the model is sensitive to the variations in the stress amplitude of the high sub-block. Comparing the life estimates obtained for the tests with $\Delta S_H/2$ of 28 and 32 MPa, a difference of about 300,000 cycles was observed. Similar results are obtained when comparing the estimates for the tests with $\Delta S_H/2$ of 36 and 40 MPa, with a difference of approximately 200,000 cycles. However, a significantly higher

difference is observed when comparing the tests with $\Delta S_H/2$ of 32 and 36 MPa, with the estimated life being about two times shorter for the test with 36 MPa. The reason for this higher difference is still unclear. Fretting fatigue tests will be performed on a later date using the loading conditions defined in Table 2. These tests will be used to investigate the capability of the model to predict the fatigue lives and if the estimated influence of the stress amplitude of the high sub-block on fatigue life is consistent with experimental results.

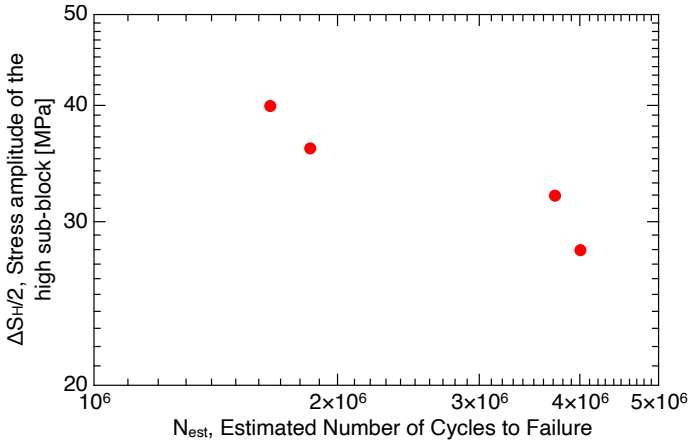

Figure 8. Stress amplitude of the high sub-block vs estimated fatigue life for the AA6201-T81 wires under variable amplitude loadings.

5. CONCLUSIONS

The fretting fatigue of 6201-T81 aluminum alloy wires taken from an AAAC (All Aluminum Alloy Cable) 900 MCM conductor under variable amplitude loading (VAL) was investigated in this study. A new set of wire/wire fatigue tests under VAL is proposed. Loading blocks formed by three sub-blocks of different amplitudes are used to represent the amplitude variations. The loading conditions defined for these tests are based on experimental-numerical data and in-field measurements taken from AAAC 900 MCM conductors. A life estimation methodology, previously used for constant amplitude loading, was extended to take into account VAL conditions. The methodology was applied to to the proposed VAL tests. The estimated fatigue lives were in a range of 1.5 to 4 million cycles. According to the life estimation methodology, the magnitude of the highest force amplitude can have a significant effect on fatigue life. In future work, fretting fatigue tests with the proposed test conditions will be performed to evaluate the accuracy of the life estimation methodology.

6. ACKNOWLEDGEMENTS

The authors would like to acknowledge the financial support of Transmissoras Brasileiras de Energia (TBE) for the project entitled *Fadiga de Cabos de Alumínio Liga (CAL) 1120 e 6201: Estudo Comparativo, Efeito de Grampos AGS e de Emendas Pré-formadas*. This project has been funded in the context of the Research and Development Program of the Brazilian National Agency of Electric Energy (ANEEL). J. A. Araújo and F. C. Castro are also grateful for the support provided by CNPq (contracts 305302/2017-5 and 307330/ 2019-2).

7. REFERENCES

Azevedo C.R.F., Cescon T., 2002. "Failure analysis of aluminium cable steel reinforced (ACSR) conductor of the transmission line crossing the Paraná River". Engineering Failure Analysis, Vol. 9, No. 6, pp. 645–664.

Azevedo C.R.F., Henriques A.M.D., Pulino Filho A.R., Ferreira J.L.A., Araújo J.A., 2009. "Fretting fatigue in overhead conductors: rig design and failure analysis of a Grosbeak aluminium cable steel reinforced conductor". Engineering Failure Analysis, Vol. 16, pp. 136–151.

Adriano V.S.R., Martínez J.M.G., Ferreira J.L.A, Araújo J.A, da Silva C.R.M., 2018. "The influence of the fatigue process zone size on fatigue life estimations performed on aluminum wires containing geometric discontinuities using the Theory of Critical Distances". Theoretical and Applied Fracture Mechanics, Vol. 97, pp. 265–278.

Baumann R., Novak P., 2017. "Efficient computation and experimental validation of ACSR overhead line conductors under tension and bending". CIGRÉ Science & Engineering, Vol. 9, pp. 5–16.

Cardou A., Cloutier L., St-Louis M., Leblond A., 1992. "ACSR electrical conductor fretting fatigue at spacer clamps". ASTM International, pp. 231–242.

Dowling N.E., Calhoun C.A., Arcari A., 2009. "Mean stress effects in stress-life fatigue and the Walker equation". Fatigue & Fracture of Engineering Materials & Structures, Vol. 32, pp. 163–179.

EPRI, 2006. "Transmission line reference book: wind-induced conductor motion". Palo Alto: Electric Power Research Institute.

Fadel A.A., Rosa D., Murça L.B., Ferreira J.L.A., Araújo J.A., 2012. "Effect of high mean tensile stress on the fretting fatigue life of an Ibis steel reinforced aluminum conductor". International Journal of Fatigue, Vol. 42, pp. 24–34.

Garcia M.A., Veloso L.A.M., Castro F.C., Araújo J.A., Ferreira J.L.A., da Silva C.R.M., 2020. "Experimental device for fretting fatigue tests in 6201 aluminum alloy wires from overhead conductors". Wear, Vol. 460–461, pp. 203448.

Goudreau S., Lévesque F., Cardou A., 2005. "Analysis of variable amplitude loading fatigue tests on overhead conductor using Palmgren-Miner rule". Sixth International Symposium on Cable Dynamics.

Kalombo R.B., Araújo J.A., Ferreira J.L.A., da Silva C.R.M., Alencar R., Capra A.R., 2015. "Assessment of the fatigue failure of an All Aluminium Alloy Cable (AAAC) for a 230 kV transmission line in the Center-West of Brazil". Engineering Failure Analysis, Vol. 61, pp. 77–87.

Lalonde S., Guilbault R., Langlois S., 2018. "Numerical analysis of ACSR conductor-clamp system undergoing wind-induced cyclic loads". IEEE Transactions on Power Delivery, Vol. 33, No. 4, pp. 1518–1526.

Matos I.M., Rocha P.H.C., Kalombo R.B., Veloso L.A.C.M., Araújo J.A., Castro F.C., 2020. "Fretting fatigue of 6201 aluminum alloy wires of overhead conductors". International Journal of Fatigue, Vol. 141, pp. 105884.

Miner M.A., 1945. "Cumulative damage in fatigue". Journal of Applied Mechanics, Vol. 67, pp. A159–A164.

Noiseux D.U., Hardy C., Houle S., 1987. "Statistical methods applied to aeolian vibrations of overhead conductors". Journal of Sound and Vibration, Vol. 113, No. 2, pp. 245–255.

Omrani A., Langlois S., Van Dyke P., Lalonde S., Karganroudi S.S., Dieng L., 2021. "Fretting fatigue life assessment of overhead conductors using a clamp/conductor numerical model and biaxial fretting fatigue tests on individual wires". Fatigue & Fracture of Engineering Materials & Structures, pp. 1–17.

Ouaki B., Goudreau S., Cardou A., Fiset M., 2003. "Fretting fatigue analysis of aluminium conductor wires near the suspension clamp: metallurgical and fracture mechanics analysis". The Journal of Strain Analysis for Engineering Design, Vol. 38, pp. 133–147.

Poffenberger J.C., Swart R.L. "Differential displacement and dynamic conductor strain". IEEE Transactions on Power Apparatus and Systems, Vol. 84, pp. 281–289.

Ramey G.E., Silva J.M., 1981. "An experimental evaluation of conductor aeolian fatigue damage mitigation by amplitude reduction". IEEE Transactions on Power Apparatus and Systems, Vol. PAS-100, No. 12, pp. 4935–4940.

Rocha P.H.C., 2019. "Studies on fatigue of two contacting wires of overhead conductors: Experiments and modeling". M.S. thesis, Department of Mechanical Engineering, University of Brasilia.

Rocha P.H.C., Díaz J.I.M., da Silva C.R.M., Araújo J.A., Castro F.C., 2019. "Fatigue of two contacting wires of the ACSR Ibis 397.5 conductor: experiments and life prediction". International Journal of Fatigue, Vol. 127, pp. 25–35.

Said J., Garcin S., Fouvry S., Cailletaud G., Yang C., Hafid F., 2020. "A multi-scale strategy to predict fretting-fatigue endurance of overhead conductors". Tribology International, Vol. 143, pp. 106053.

Susmel L., Taylor D., 2007. "A novel formulation of the Theory of Critical Distances to estimate lifetime of notched components in the medium-cycle fatigue regime". Fatigue & Fracture of Engineering Materials & Structures, Vol. 30, pp. 567–581.

Susmel L., Taylor D., 2012. "A critical distance/plane method to estimate finite life of notched components under variable amplitude uniaxial/multiaxial fatigue loading". International Journal of Fatigue, Vol. 38, pp. 7–24.

Steier V.F., Doca T., Araújo J.A., 2018. "Fretting wear investigation of 1350-H19 aluminum wires tested against heat treated surfaces". Wear, Vol. 415–415, pp. 1–8.

Zhou Z.R., Cardou A., Goudreau S., Fiset M., 1994. "Fretting patterns in a conductor-clamp contact zone". Fatigue & Fracture of Engineering Materials & Structures, Vol. 17, No. 6, pp. 661–669.

8. RESPONSIBILITY NOTICE

The authors are the only responsible for the printed material included in this paper.